Comput Sci Res Dev
DOI 10.1007/s00450-010-0137-x

SPECIAL ISSUE PAPER

Discriminative Generalized Hough transform for localization of joints in the lower extremities

Heike Ruppertshofen · Cristian Lorenz · Sarah Schmidt · Peter Beyerlein · Zein Salah · Georg Rose · Hauke Schramm

© Springer-Verlag 2010

Abstract A fully automatic iterative training approach for the generation of discriminative shape models for usage in the Generalized Hough Transform (GHT) is presented. The method aims at capturing the shape variability of the target object contained in the training data as well as identifying confusable structures (anti-shapes) and integrating this information into one model. To distinguish shape and anti-shape points and to determine their importance, an individual positive or negative weight is estimated for each model point by means of a discriminative training technique. The model is built from edge points surrounding the target point and the most confusable structure as identified by the GHT. Through an iterative approach, the performance of the model is gradually improved by extending the training dataset with images, where the current model failed to localize the target point. The proposed method is successfully tested on a set of 670 long-leg radiographs, where it achieves a localization rate of 74–97% for the respective tasks.

H. Ruppertshofen (✉) · H. Schramm
Institute of Applied Computer Science, University of Applied Sciences Kiel, Kiel, Germany
e-mail: heike.ruppertshofen@fh-kiel.de

C. Lorenz
Department Digital Imaging, Philips Research Europe, Hamburg, Germany

S. Schmidt · P. Beyerlein
Department of Engineering, University of Applied Sciences Wildau, Wildau, Germany

H. Ruppertshofen · S. Schmidt · Z. Salah · G. Rose
Institute of Electronics, Signal Processing and Communication Technology, Otto-von-Guericke-University, Magdeburg, Germany

Keywords Object localization · Generalized Hough transform · Discriminative training · Optimal model generation

1 Introduction

Many applications in the area of computer-aided diagnosis are in need of object localization prior to execution in order to run fully automatically. In this paper, we will describe a general method for automatic object localization, i.e. locating one target point representing the object of interest, utilizing the GHT; thereby focusing on the task of joint localization in lower limb radiographs as a prerequisite for orthopedic applications. Among these are automatic measurements of length and angles of bones or automatic segmentations, which are necessary for bone density estimation as well as pre-operative planning, as described by Gooßen et al. [6]. Often, the required positions are still determined manually, which is time-consuming, potentially inconsistent and often presupposes expert knowledge. These challenges are evaded by the employment of automatic localization procedures, which furthermore have the advantage that the results are reproducible and independent of the operator.

In literature, different methods for automatic object localization have been presented. Many of these are tailored for the specific localization task at hand making use of anatomical knowledge in combination with, e.g., gray-value thresholding and morphologic operators [8], which in many cases still require expert knowledge.

More general approaches are given by gray-value based approaches such as template matching [10] or atlas-based registration [16]. These procedures, however, are not applicable for tasks, where one cannot rely on the gray-value profile of the target object due to contrast agents

Published online: 14 October 2010

or artificial replacements. Heimann et al. [7] proposed to use evolutionary algorithms to estimate the pose of a target object. Thereby the shape population is initialized with the mean pose parameters of the target objects in the training images. This approach becomes unfeasible in case of varying fields of view, since the position of the target object differs relative to the image size. Another option is the usage of marginal space learning [17], which determines the object position and further pose parameters iteratively using Haar wavelet and steerable features.

Despite presumed long processing times, we want to focus on the GHT [1] as means of object localization. The advantage of the GHT is that it is robust towards image noise and occlusions or missing object parts, which renders it interesting for medical applications, especially in case of pre- and post-operative image acquisitions or the presence of artificial replacements. The execution of the GHT can be separated into two types based on the kind of model which is used to represent the target object. Different groups [4, 11, 12] use appearance models based on codebooks of image patches. The second approach is to employ point models representing the shape of the object [13–15]. Codebooks of image patches are mainly used for the localization of objects in cluttered scenes and rely on gray-value appearances. Medical images are clearly arranged and the objects displayed are often well represented by their shape, therefore we prefer the faster and for our task better suited shape models.

In order to improve the localization accuracy of the GHT and to speed up the procedure, we employ the training of slim, discriminative models, which contain the variability of the object expressed in the data as well as information about rivaling objects (anti-shapes), which resemble the object of interest. To this end, each model point is equipped with an individual weight, relative to its importance. This approach has also been followed by Deselaers et al. [3] and Maji and Malik [12]; yet they do not allow for negative weights, which we employ to represent anti-shapes. This approach results in models, which are discriminative for the target object, and therefore reduce false-positive rates. Through an iterative training of model points and weights, it is possible to capture the variability of the target object such that the sole estimation of object position is sufficient for a successful localization. Rotation and scaling of the model do not need to be considered; thus decreasing processing time. Furthermore, the procedure is not in need of prior shape or appearance information about the target object, whereby it runs fully automatically and is applicable to detect arbitrary objects.

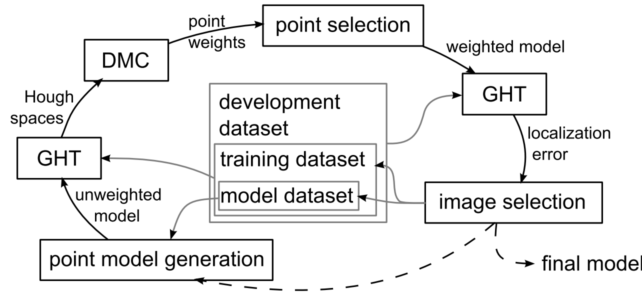

Fig. 1 Overview of the iterative training procedure for creation of discriminative models utilizing the Generalized Hough Transform (GHT) and a discriminative training procedure (DMC) as described in Sect. 2

2 Methods

The proposed method for model generation consists of two main modules: the GHT for object localization to establish the necessary shape information and a discriminative training procedure (DMC) [2] to estimate model point weights for an ideal combination of this information. The building process of the models runs iteratively so that shape and anti-shape variability contained in the dataset is successively identified and included into the model. Thereby, the set of training images is extended in each iteration by appending images where the current model performed badly. A general overview of the procedure is given in Fig. 1; the individual modules are explained in the following sections.

2.1 Model generation and iterative model training

The aim of the iterative supervised training is to create models which capture the variability of the target object in the dataset and to determine the importance of shape and anti-shape points without the incorporation of expert knowledge or user interaction.

To this end a number of images are chosen, forming the development dataset, which is used to generate a model and to monitor its performance. This dataset should contain representative characteristics of the target object to be able to create a discriminative, but yet general model of the target object. Part of the development images make up the training dataset on which the model point weights are determined. This dataset contains a further subset, which is utilized to generate new model points. Not all training images are integrated into the model generation to avoid overfitting effects and to reduce model size.

At the beginning of the procedure an initial meaningful model is created using the approach shown in Fig. 2. A region of interest of given size is extracted around the target point from the images of the model dataset. By employing these regions of interest for model creation, the neighborhood of the target point is included into the model as well, which in many cases contains significant information for the

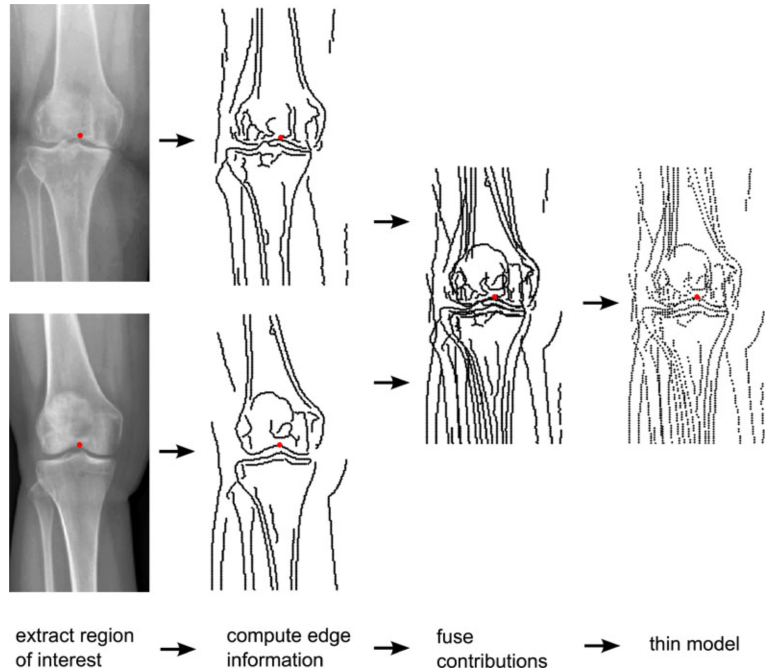

Fig. 2 (Color online) Processing chain for model generation. First a region of interest is extracted from the images from which the edges are extracted. These intermediate models are fused to create the final model, which is furthermore thinned as to increase the entropy of each model point. The target point in the lower part of the femur is shown as (*red*) dot

localization task. On these extracts, edge points are computed and fused to form the initial shape model. Through this approach shape variability of the target object is included, as becomes obvious in Fig. 2; here especially visible for the angle of the femur. In the last step, the model is thinned to guarantee that each model point carries exclusive shape information to keep its size small while at the same time increasing the entropy of the model. This step is to ensure that the generated model is compatible with the training algorithm described in Sect. 2.3, which weights the points according to their importance. Points which carry the same information content are considered less important and are thereby downgraded. As thinning criteria, the distance and difference in gradient directions of model points are considered such that they do not leave the same voting trace in the Hough space.

Since the processing time of the GHT depends on the size of the model, a further point selection is performed after each training step including the GHT and DMC. Thereby, the model size is reduced by rejecting points which obtained low absolute weights and therefore do not have a large impact in the GHT.

The trained weighted model is finally tested on the development dataset. Thereafter the set of training and model images is extended with a fixed number of images where the current model performed poorly, meaning that a high localization error was observed. Using these new images, the model is extended by adding new points, again using the method shown in Fig. 2. By this method, the model would consist exclusively of shape information. To be able to incorporate anti-shape information as well, a second region is extracted around the location which obtained the highest vote in the GHT and therefore contains the strongest rivaling object. During the next training iteration, these points will most likely be assigned negative weights, repelling the model from the anti-shape location.

Once the model is able to successfully localize the target object in all images of the development dataset or a maximal number of iterations is reached, the procedure ends.

2.2 Generalized Hough transform

The GHT is a model-based method for object localization, which has been introduced by Ballard [1] as an extension of the standard Hough transform for lines or circles. The method is capable of localizing objects of known arbitrary shape and is insusceptible against occlusion or image noise, which renders it very interesting for medical image processing.

The localization procedure operates by transforming the given image into a parameter space, the so-called Hough space, where each cell represents a certain model transformation. In our case, only translation is considered; however, a full affine transformation would be conceivable, but is computationally expensive.

For the localization procedure, a point model representing the shape of the target object is needed. This model consists of the coordinates of model points relative to a reference point (as shown in Fig. 2) and the gradient (or surface normal) direction at each point. The model points are stored in a so-called R-table where they are grouped according to their gradient direction for faster access during the voting procedure described in the following.

To perform the localization, the edge image is computed, using, e.g., the Canny edge detector. For each edge point, the model points with a similar gradient direction are obtained from the associated R-table bin. Assuming that the model point m_k coincides with the edge point e_j the corresponding possible object location is determined through $c_i = e_j - m_k$ and the vote in the Hough cell c_i is incremented. In the end, the Hough cell with the highest number of votes is returned as the most likely object position.

If further transformation parameters like scaling or rotation are of interest, the model needs to be transformed accordingly and the procedure is repeated. This however results in much longer processing times and a higher dimensional Hough space. Since the differences in size and angle of medical objects are comparably small, we follow the approach to include this variability into our model, as described in the previous section, to reduce computational effort.

In the process of model training, the GHT is first performed using an unweighted model where each model point casts a vote of 1, to obtain the information content of the current model. This information is exploited in the training procedure described in the next section to determine model point weights for an optimal combination of the available information. When employing the GHT for object localization, a weighted model is utilized, where each model point votes with its individual weight such that they have unequal impact on the localization result. The determined model point weights can have positive as well as negative values. Thereby, the positive weights belong to shape points, while anti-shape points are allocated negative weights.

2.3 Training of model point weights

The DMC technique [2], which we employ for training of model point weights, is a machine learning technique, which aims at an optimal probabilistic combination of different knowledge sources into one model.

To deduce the training procedure, we employ a probabilistic view of the Hough space by transforming it into a probability mass function. This is achieved through normalization of the number of votes N_i in each Hough cell c_i by the total number of votes N. Thereby, we obtain a posterior probability for each possible object location (represented by the Hough cells) given an image X:

$$p(c_i|X) = \frac{N_i}{N}. \tag{1}$$

Instead of searching for the cell with the highest number of votes, the result of the GHT can now also be obtained by determining the Hough cell with the highest posterior probability.

Dividing the Hough space into the separate contributions from the individual model points, a model point dependent posterior probability is established for each model point m_j:

$$p_j(c_i|X) = \frac{N_{ij}}{N_j}. \tag{2}$$

Since the posterior probabilities defined in (2) cannot solely be used for object localization, a suitable combination of these knowledge sources needs to be found. Following the Maximum-Entropy principle introduced by Jaynes [9] the optimal incorporation of model point information is given via a log-linear combination:

$$p_\Lambda(c_i|X) = \frac{\exp(\sum_j \lambda_j \cdot \log p_j(c_i|X))}{\sum_k \exp(\sum_j \lambda_j \cdot \log p_j(c_k|X))}. \tag{3}$$

The coefficients $\Lambda = \{\lambda_j\}_j$ regulate the influence of each model point posterior probability $p_j(c_i|X)$ on the model combination $p_\Lambda(c_i|X)$. The value of λ_j is therefore related to the importance of the model point m_j and will be interpreted as model point weight.

To estimate the model point weights from (3) with respect to a minimal localization error on training images, an error function E is defined:

$$E(\Lambda) = \sum_n \sum_i \varepsilon(\tilde{c}_n, c_i) \frac{p_\Lambda(c_i|X_n)^\eta}{\sum_k p_\Lambda(c_k|X_n)^\eta}. \tag{4}$$

The function accumulates the weighted error over all images X_n. Thereby, the Euclidian distance ε of the correct object position $\tilde{c}_n$ and a Hough cell c_i is chosen as error measure, which is weighted with an indicator function comprised of the posterior probabilities. The exponent η in the indicator function regulates the influence of rivaling hypotheses c_k on the error measure. The error function is designed in a way that in a cell distant of the true solution a large probability is penalized stronger than a small one. The true cell, which holds no error, can have the highest probability without adding to the overall error.

For the determination of optimal λ_j, which minimize the error function in (4), a gradient descent scheme is explored. Due to the high dimensional search space and the most likely not convex error function, the existence of a global minimum and therefore its determination cannot be guaranteed. However, the usage of model point weights resulting from a local minimum already significantly increase the localization accuracy of the model as can be seen in Sect. 4.

3 Experimental setup

3.1 Material and task

The procedure is tested on a dataset of 670 long-leg radiographs of adult patients with varying field of view. Most

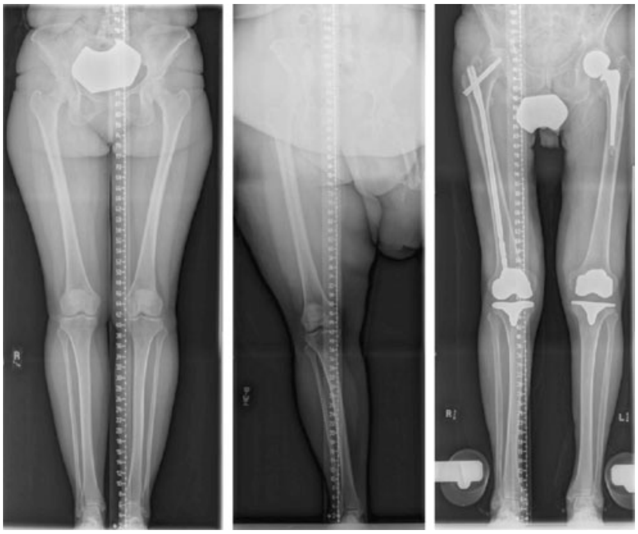

Fig. 3 Examples from the dataset of long-leg radiographs

images cover both legs from hip to ankle, while some images show only one leg or certain joints. Different artificial replacements of the hip or knee are visible as well as fractures or further medical conditions. The images were stitched together from up to three images using the procedure described by Gooßen et al. [5]. In Fig. 3 a few examples of the database are displayed to demonstrate the diversity of the images. Furthermore, Fig. 4 shows exemplary extracts of the right knee.

The images have an isotropic resolution of 0.143 mm. In order to reduce processing time the images were downsampled to a resolution of 1.14 mm. As edge detector the Matlab[1] implementation of the Canny method is utilized, which automatically determines the thresholds from the gradient image and applies a sigma of 1 as the standard deviation of the Gaussian filter.

The localization is performed for the three joints: hip, knee and ankle. The results will be integrated in the segmentation procedure described by Gooßen et al. [6] for an initial placement of the models.

To evaluate the accuracy of the automatic localization, one observer annotated target points for all joints, which are used as ground-truth. As target point a salient landmark on the boundary of the target object was chosen, which could be reliably annotated by the observer in all images. The mean intra-observer error for the annotations, which were determined in two passes for all target points, adds up to 2.3 mm for the hip, 1.3 mm for the knee and 2.6 mm in case of the ankle.

[1] Version 7.6.0.324 (R2008a), MathWorks, Natick, MA, USA.

3.2 Design of experiments

The training procedure will be employed to generate discriminative models for the right joints only. For the localization of the left joints the mirrored model can be used, since there are no significant differences between right and left joints.

Prior to the training procedure, about 60 images without pathological findings for the joint of interest were chosen at random as development dataset. From these, three images were taken, which form the initial training dataset. One of these images is furthermore utilized for model generation.

After each training step, the three images with the largest localization error are determined and added to the set of training images. Through this proceeding a set of images, which are needed to characterize the given dataset and to capture the underlying variability, is established. New model points are extracted from the image with the largest error as described in Sect. 2.1.

The training stops if an error of less than 5 Hough cells, which have a spacing of 2.29 mm, is obtained on all images of the development dataset or if no further improvement is achieved.

In the end, the models are tested on the left and right joints of the complete dataset yielding the results shown in the next section.

4 Results

The evolution of the models is shown exemplarily in Table 1 for the case of the knee, which needs 4 iterations to converge. As can be seen there, the number of model points increases in each iteration resulting in a more and more discriminative model demonstrated by the decreasing error rate and number of misclassifications on the development dataset.

In case of the knee, the strongest anti-shape is the knee of the opposite leg, which appears quite similar when regarded without the fibula. While the initial model localized only 44 of 51 knees, from which only 32 are right knees, the final model has a localization rate of 100%. Eventually, a model evolved which represents the target object, captures its variability and is capable of distinguishing it from anti-shapes.

In case of the hip 5 iterations are needed to create a meaningful model, while the ankle, which seems to be the most difficult object, probably due to its rotational freedom, needs 6 iterations. The final models are shown in Fig. 5. To relate the model points to the object structures, they are superimposed on an example image. Furthermore, the model points are color-coded relative to their weight to be able to distinguish shape and anti-shape points and to determine their importance. Model points with negative weights make up about 25–40% of the models.

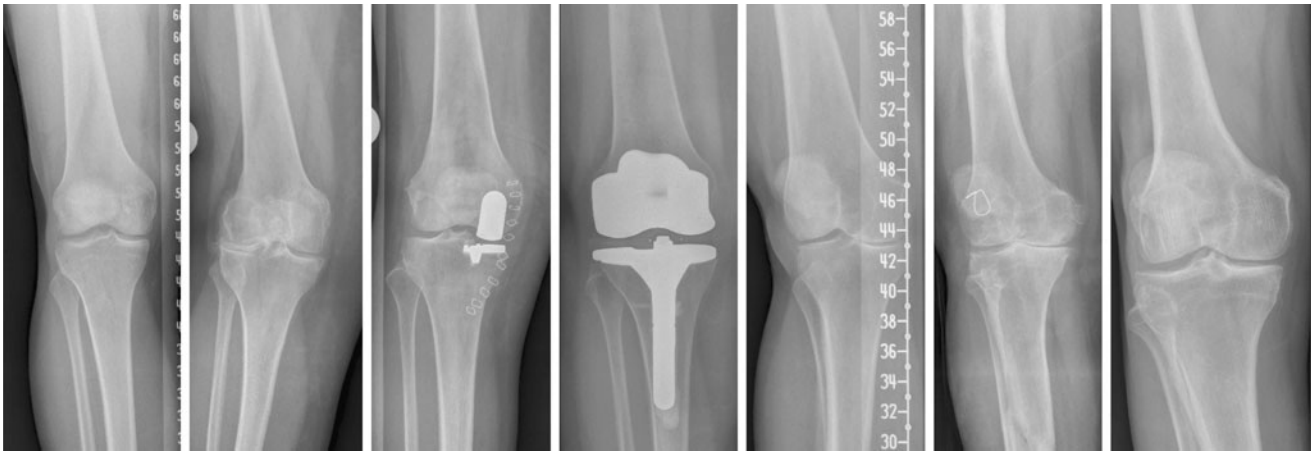

Fig. 4 Exemplary extracts of the right knee, showing the diversity visible in the dataset. The images exhibit differences in the rotational angle, size of the joint and the visibility of the fibula. Furthermore, disturbing objects like the ruler or implants may occur

Table 1 Evolution of the knee model. In the top part of the table the number of training images and the size of the trained model is specified. The middle part states the mean error in mm on the training and development images. In the bottom part the number of right or left legs, which were localized by the current model, are listed

Iteration	1	2	3	4
No. of training images	3	6	9	12
No. of model points	75	555	1817	1923
Error on training data	1.7	2.1	3.3	1.6
Error on development data	97.5	25.2	24.8	3.4
Right knees localized	32	48	48	51
Left knees localized	12	2	1	0

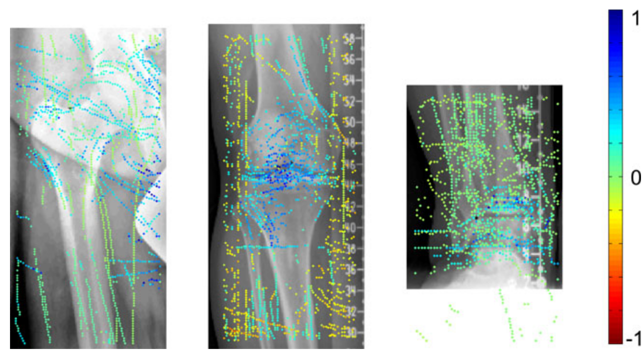

Fig. 5 (Color online) The final models resulting from the training procedure are shown superimposed on an example image. The model points are color-coded relative to their weight. *Blue* color represents a weight of 1, while *red* represents a weight of -1

Table 2 Results of the localization task for the three joints. Stated is the size of the respective model and the mean error of the successful localizations in mm divided by the state of the joint

	Model size	Normal	Replacement	Anomaly
Hip	1608	12.5	14.6	17.4
Knee	1923	4.3	8.5	6.8
Ankle	1187	9.8	–	13.3

The hip model contains mainly strong shape points, which represent different sizes of the femoral head and different angles of the shaft position. The same holds true for the ankle model, which concentrates on the gap between tibia and talus, which is the most robust part with only little inter-patient variance. The model points which extend below the image border belong to anti-shapes, among others the upper part of the tibia. In case of the knee, the model focuses on the gap between femur and tibia, while also containing strong anti-shapes in the region where the fibula of the opposite leg would be.

In all models, horizontal or vertical chains of model points can be seen, which most likely originated from the ruler, the image boundary or artifacts introduced by the stitching algorithm. These model points do not contain important information for the object location, nor are they reliable anti-shape points. Therefore, further research will aim at the elimination of these points to obtain slim models without redundant information.

The localization performance of the generated models can be seen in Table 2 and the chart in Fig. 6. For a fair comparison, the images are sorted into three categories, namely images with artificial replacements, with pathological findings and the remaining images where the joints do not exhibit any abnormalities. The latter images make up about 93%, 75% and 96,% of the dataset in case of the hip, knee and ankle, as can also be estimated from Fig. 6.

The knee has the best localization rate of 97% in case of the normal joints, followed by the ankle with 87%. The hip

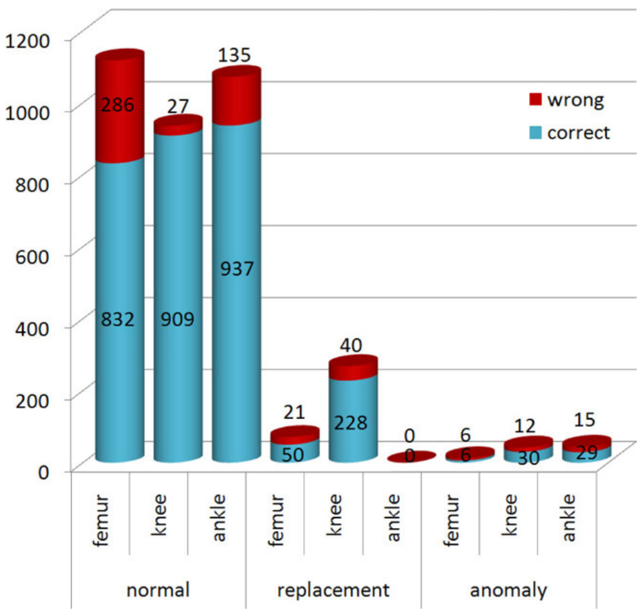

Fig. 6 Number of successfully or failed localizations of the hip, knee and ankle on the unknown test data. Results are separated based on the state of the joint, which can be normal, with artificial replacement or with pathological findings; results for right and left joints are combined

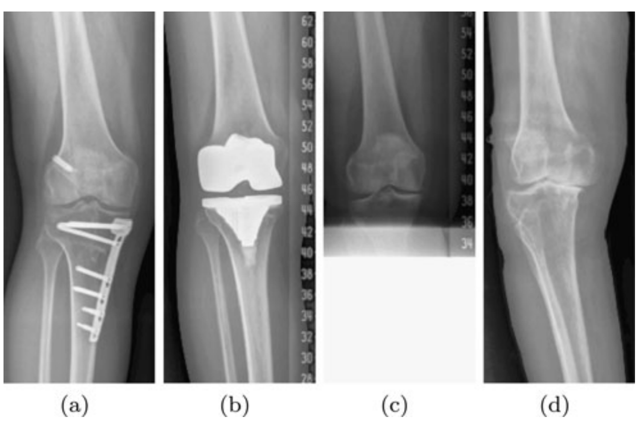

Fig. 7 Extracts of difficult images where the localization succeeded: (**a**) implant, (**b**) artificial replacement, (**c**) constrained field of view, (**d**) shifted knee joint and occluded fibula

achieved the lowest rate with only 74%. The low localization rate of the hip is due to an often very low image contrast in that region, which impairs its delineation even for a human observer. A localization was considered successful if an error of less than 1 cm was achieved, which is the capture range of the segmentation procedure described in Gooßen et al. [6].

Since the models were trained on healthy images, the correct localization of joints containing artificial replacements and abnormalities cannot be premised. Yet, in case of the knee a localization rate of 85% and 71% is achieved on these images, respectively. In Fig. 7 extracts of example images are displayed where the localization of the right knee was

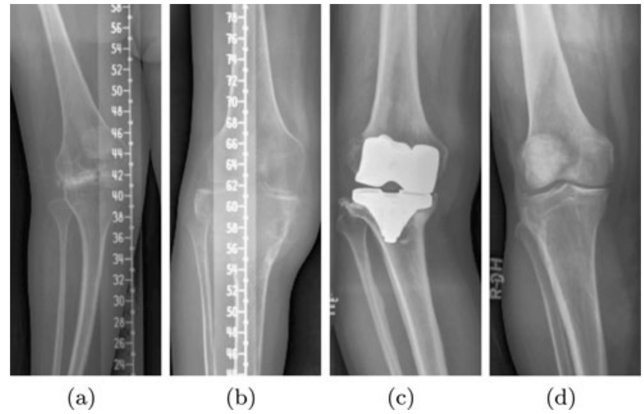

Fig. 8 Extracts of example images where the localization failed

successful, although the task was difficult. Figure 8 shows examples where the localization failed.

To motivate the usage of model point weights, further experiments have been conducted for the knee localization to compare our approach with a standard unweighted GHT. For this purpose, 100 random images without pathological findings of the knee were chosen. The results of the following two experiments are compared to the previous one (stated as experiment 0) in Table 3.

In the first experiment, an initial model was created from the four model images, which were determined by the iterative procedure. This model should contain sufficient information to localize all joints correctly since it is a superset of shape points of the weighted knee model created by the previous experiment, which has a localization rate of 96%. Yet, when employing this unweighted model, the correct knee was localized in only 49% of the images, with a mean localization error of 8.8 mm.

In the second experiment, the trained weighted model was employed, with anti-shape points and weights excluded. This model achieved a localization rate of 91%, but with a larger mean error of 7.1 mm compared to the weighted model.

Apart from yielding a higher localization rate and a lower mean error, the weighted model also generates a clearly arranged Hough space with a definite maximum as can be seen in Fig. 9. This result is more robust and reliable than the other two, although all experiments yield about the same result in the displayed case.

5 Discussion

We presented an approach for generation of discriminative shape models and object localization by means of the GHT. The attractiveness of the introduced procedure lies in the fully automatic application flow and the straightforward

Table 3 Comparison of the weighted model (experiment 0) with the standard GHT employing a large unweighted model (1) and a thinned unweighted model (2). Compared are the size of the model, the mean localization error in mm, and the percentage of correct localizations

Experiment	0	1	2
No. of model points	1923	2926	1135
Mean localization error	3.7	8.8	7.1
Correct localizations	96	49	91

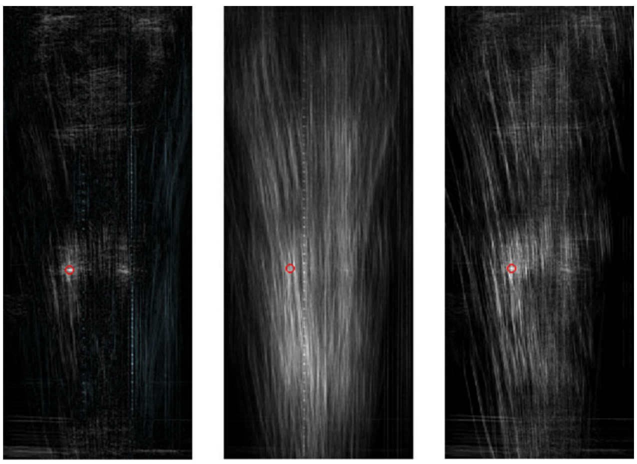

(a) weighted model (b) untrained model (c) unweighted model

Fig. 9 Comparison of the Hough spaces obtained in the three experiments. The red circles indicates the location of the target point. Shown are the Hough space obtained with (**a**) the weighted model, (**b**) the untrained model from experiment 1 and (**c**) the unweighted model from experiment 2

handling. For the generation of suitable models, only a number of images with annotated target points and a defined region of interest, from which the model points are to be extracted, are needed. The procedure, which can be applied to localize arbitrary objects that are well defined by their shape, was successfully employed to localize the joints of the lower limb.

The trained models achieve a localization rate of 74–97% for the different tasks with a mean localization error of 4.3–12.5 mm, which is remarkable considering the low resolution of 2.29 mm employed in the GHT. In many cases of a wrong localization result, the second or third highest vote in the Hough space points to the correct joint, such that a localization rate of more than 90% could be obtained by keeping multiple candidates. Although, images with artificial replacements, fractures and further pathological findings have not been included in the training set, the robustness of the generated models allows for localizing almost 70% of those cases.

The experiments demonstrated the feasibility to incorporate the variability of the target object visible in the training images as well as anti-shape structures into one shape model. This is achieved through an iterative training procedure, which successively improves the model performance by adding images, where the current model yields wrong localizations, to the set of training images. Through the obtained shape models the false-positive rates are reduced, while also shortening processing time, since the GHT has to be run only once and rotation and scaling do not need to be considered.

The necessity of model point weights was proven in further experiments, which revealed that the sole usage of contour information is not sufficient for object localization in our case. In fact, the determination and weighting of robust model points is of high importance to increase localization accuracy and reduce false-positive rates. Establishing this information by hand is a difficult and time-consuming task, which would require substantial expert knowledge.

The current experiments were run on down-sampled images to reduce processing time. The achieved accuracy is sufficient for the given task of model initialization for segmentation procedures as utilized by Gooßen et al. [6]. If a higher accuracy is needed, the procedure could be embedded into a multi-level setting.

Acknowledgements The authors would like to thank the Dartmouth-Hitchcock Medical Center and Digital X-Ray, Philips Healthcare for providing the radiographs used in this study. This work is partly funded by the Innovation Foundation Schleswig-Holstein under the grant 2008-40 H.

References

1. Ballard DH (1981) Generalizing the Hough transform to detect arbitrary shapes. Pattern Recogn 13(2):111–122
2. Beyerlein P (1998) Discriminative model combination. In: IEEE international conference on acoustics, speech and signal processing. IEEE Press, New York, pp 481–484
3. Deselaers T, Keysers D, Ney H (2005) Improving a discriminative approach to object recognition using image patches. In: 27th annual symposium of the German association for pattern recognition. LNCS, vol 3663. Springer, Heidelberg, pp 326–333
4. Gall J, Lempitsky V (2009) Class-specific Hough forests for object detection. In: IEEE conference on computer vision and pattern recognition. IEEE Press, New York
5. Gooßen A, Schlüter M, Pralow T, Grigat RR (2010) A stitching algorithm for automatic registration of digital radiographs. In: International conference on image analysis and recognition. LNCS, vol 5112. Springer, Heidelberg, pp 854–862
6. Gooßen A, Hermann E, Gernoth T, Pralow T, Grigat RR (2010) Model-based lower limb segmentation using weighted multiple candidates. In: Bildverarbeitung für die Medizin. Springer, Berlin, pp 276–280
7. Heimann T, Münziger S, Meinzer HP et al (2007) A shape-guided deformable model with evolutionary algorithm initialization for 3D soft tissue segmentation. In: International conference on information processing in medical imaging, pp 1–12
8. Heimann T, van Ginneken B, Styner M et al (2009) Comparison and evaluation of methods for liver segmentation from CT datasets. IEEE Trans Med Imaging 28(8):1251–1265
9. Jaynes ET (1957) Information theory and statistical mechanics. Phys Rev 106(4):620–630

10. Lee Y, Hara T, Fujita H, Itoh S, Ishigaki T (2001) Automated detection of pulmonary nodules in helical CT images based on an improved template-matching technique. IEEE Trans Med Imaging 20(7):595–604
11. Leibe B, Leonardis A, Schiele B (2008) Robust object detection with interleaved categorization and segmentation. Int J Comput Vis 77(1–3):259–289
12. Maji S, Malik J (2009) Object detection using a max-margin Hough transform. In: IEEE conference on computer vision and pattern recognition. IEEE Press, New York, pp 1038–1045
13. Recuero ABM, Beyerlein P, Schramm H (2008) Discriminative optimization of 3D shape models for the Generalized Hough transform. In: AMIES Kiel
14. Ruppertshofen H, Lorenz C, Beyerlein P, Salah Z, Rose G, Schramm H (2010) Fully automatic model creation for object localization utilizing the Generalized Hough transform. In: Bildverarbeitung für die Medizin. Springer, Berlin, pp 281–285
15. Schramm H, Ecabert O, Peters J et al (2006) Towards fully automatic object detection and segmentation. In: SPIE medical imaging 2006: image processing, p 614402
16. Seghers D, Slagmolen P, Lambelin Y et al (2007) Landmark based liver segmentation using local shape and local intensity models. In: MICCAI workshop on 3D segmentation in the clinic: a grand challenge. Springer, Berlin, pp 135–142
17. Zheng Y, Georgescu B, Comaniciu D (2009) Marginal space learning for efficient detection of 2D/3D anatomical structures in medical images. In: 21st international conference on information processing in medical imaging. LNCS, vol 5636. Springer, Heidelberg, pp 411–422

Heike Ruppertshofen is a Ph.D. student in her second year at the University of Applied Sciences Kiel and the University of Magdeburg in Germany. The emphasis of her thesis is object localization and classification in medical images. Heike received her Master's Degree in Image Processing from the University of Lübeck, Germany in 2009.

Cristian Lorenz studied physics in Freiburg and Hamburg (Germany). After receiving his diploma degree in 1990 he was a graduate student at the Hamburg Synchrotron Radiation Laboratory (HASYLAB). For his work on experimental atomic physics, especially electron and soft X-ray spectroscopy of vaporized metals, he obtained his doctoral degree in 1993. Since 1993 he works as scientist at the Philips Research Laboratories in Hamburg in the field of medical image processing. His main research interests are statistical and functional organ models and model based image analysis.

Sarah Schmidt is a research assistant at the Bioinformatics Laboratory of the Technical University of Applied Sciences (TUAS) Wildau since 2009. Her field of study is the development of algorithms for the automatic Phytoplankton detection from fresh water microscopy images. In doing so, she applies and enhances the DMC method. Sarah received a Master's Degree in Biosystems Engineering/ Bioinformatics from the TUAS Wildau in 2009.

Peter Beyerlein is a professor for bioinformatics, signal processing and mathematics and head of a Bioinformatics Laboratory at the Technical University of Applied Sciences (TUAS) Wildau since 2006. He is involved in the international research community of signal processing and machine learning. Peter holds a Ph.D. in computer science from the RWTH Aachen since 2000.

Zein Salah is currently a senior researcher at the Department of Electronics, Signal Processing and Communications and the Department of Simulation and Graphics, University of Magdeburg, Germany. He received a Ph.D. degree in computer science from the University of Tübingen, Germany, in 2006. His research focus is on medical image processing, visualization, and augmented reality.

Hauke Schramm studied communications engineering at the University Kiel and received his Ph.D. from the RWTH Aachen in the field of automatic speech recognition. For 10 years he has worked as scientist and project leader in the Philips Research Laboratories in Aachen. Since 2007 he is professor for information technology at the University of Applied Sciences Kiel. In this position, he supervises, among other topics, projects concerning the automatic analysis of medical and industrial image data.